

PAPER • OPEN ACCESS

## Design and Implementation of Microstrip Patch Ultra-wide Band Antenna for Detection of UHF Partial Discharge

To cite this article: Z Nawawi *et al* 2019 *IOP Conf. Ser.: Mater. Sci. Eng.* **602** 012001

View the [article online](#) for updates and enhancements.



**240th ECS Meeting** ORLANDO, FL

Orange County Convention Center Oct 10-14, 2021

Abstract submission due: April 9

SUBMIT NOW

# Design and Implementation of Microstrip Patch Ultra-wide Band Antenna for Detection of UHF Partial Discharge

Z Nawawi<sup>1</sup>, M A B Sidik<sup>1</sup>, M I Jambak<sup>1</sup>, N Ahmad<sup>2</sup>, M H Ahmad<sup>2</sup>, C L G P Kumar<sup>2</sup>, E P Walidi<sup>3</sup>, and Aulia<sup>3</sup>

<sup>1</sup>Department of Electrical Engineering, Universitas Sriwijaya, Palembang, Indonesia.

<sup>2</sup>Institute of High Voltage & High Current, School of Electrical Engineering, Universiti Teknologi Malaysia (UTM), Johor Bahru, Malaysia.

<sup>3</sup>Department of Electrical Engineering, Faculty of Engineering, Universitas Andalas, Padang, Indonesia.

E-mail: mohdhafizi@utm.com.my

**Abstract.** Partial discharge (PD) is an electrical release or spark that occurs between two conducting electrodes that are not bridging, and it can occur at any points in the insulation system. PDs emit electromagnetic field radiation in the frequency range of 300 MHz to 1.5 GHz. Thus, it is more appropriate to detect and monitor partial discharge using an ultra-wideband antenna which offers more accuracy than the narrowband antenna. This paper proposes the design and implementation of a microstrip patch antenna which has been designed to possess wider detection performance of ultra-high frequency (UHF) PD signal. The PD spectra of the designed UWB antenna and the commercial whip antenna was compared and analyzed. The result shows that the UWB antenna can effectively detect the UHF PD signals that occur between two electrodes. As results, it is implied that PD measurement by using designed UWB antenna is found to suitable to detect the PD signals for online monitoring of high voltage equipment.

## 1. Introduction

PD will cause energy loss and insulation degradation incrementally. Hence, PD detection methods are used to verify if any partial discharge sources begin to develop or exist in the insulating systems. Presently, there are two types of PD detection methods, non-conventional method and the conventional method [2], [3]. Non-conventional methods consist of optical, ultra-high frequency detection and acoustic whereas conventional methods consist of electrical methods such as impedance matching and the coupling capacitor. The method of a coupling capacitor for partial discharge detection is accurate but requires direct electrical connection to the coupling capacitor with the test system which is an offline test at a laboratory.

UHF PD signal detection can be used to diagnose the insulation condition for the power cable, cable end-terminations, surge arrester, transformer and gas insulated switchgear (GIS). The range of frequency generated between 300 MHz to 3 GHz is known as UHF that generated by PD. PD occurred within the duration of nanoseconds, and it can be detected by using sensors. In power cable, the signals travel inside to have a very strong attenuation of PD pulses within a high-frequency spectrum. The apparent charge must be less than 10 pC for the acceptance level of PD in power cable [4]. Then,



UHF PD detection method has a high sensitivity, wide detection range and reduce external noise in the application of GIS. In GIS, the PD current pulse has a short rise time which is less than 100 picoseconds in sulfur hexafluoride (SF6).

Generally, the UHF method is one of the most prominent detection method used in detecting insulation defects in high voltage equipment. The UHF detection method has the advantages of high sensitivity, great immunity against electrical noise and very efficient for localization of PD and identification of PD source even for low level discharges hidden inside the insulation [1]. Compared with the antenna in communication systems, the UHF antenna detects the electromagnetic waves in the frequency range from 300 MHz to 3 GHz.

However, the UHF antenna for partial discharge detection in high voltage equipment is not enough because the antennas either have narrow operating bandwidths or have low gain. Therefore, there has been growing interest in introducing an antenna with wider bandwidth and higher gain, which is used for UHF PD online monitoring in high voltage equipment [5]. Thus, a UWB microstrip patch antenna for online monitoring of partial discharge in high voltage equipment is proposed in this paper. The UWB antenna plays an important role in the accuracy and sensitivity of the PD detection system. A UWB antenna should have a higher gain because the PD signals in high voltage equipment are weaker and have attenuation due to several refraction and reflection.

In this paper, UWB antennas were designed and fabricated for a partial discharge detection. Then, the UWB antennas were used to measure UHF partial discharge in high voltage laboratory.

## 2. Antenna Design

A patch antenna consists of the ground plane, radiating patch, and substrate. The ground plane is at the bottom surface of the substrate while the radiating patch is on the top surface of the substrate. Radiating patch will act as a resonant cavity, where the short circuit will occur at both the top and bottom surfaces, and the open circuit will occur on the other sides.

The parameters of the microstrip patch antenna such as the width and length of the patch, the substrate can be calculated by using the microstrip patch antenna formula. Figure 1 shows the geometry of the microstrip patch antenna.

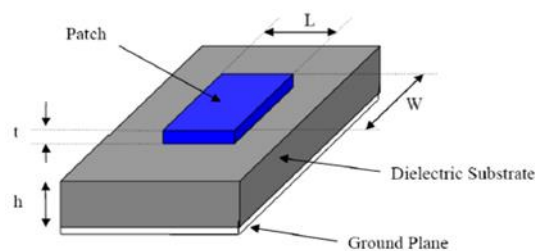


**Figure 1.** The basic element of the microstrip patch.

The width radiating patch is calculated as

$$W = \frac{c}{2f_o \sqrt{\frac{\epsilon_r + 1}{2}}} \quad (1)$$

The effective dielectric constant to find the length of the microstrip patch is calculated using the following equation

$$\epsilon_{\text{reff}} = \frac{\epsilon_r + 1}{2} + \frac{\epsilon_r - 1}{2} \left( 1 + 12 \frac{h}{W} \right)^{-\frac{1}{2}} \quad (2)$$

The effective length is calculated by

$$L_{\text{eff}} = \frac{c}{2f_o \sqrt{\epsilon_{\text{reff}}}} \quad (3)$$

Effective length due to fringing effects,  $\Delta L$  is calculated as

$$\Delta L = 0.412h \frac{(\epsilon_{\text{reff}} + 0.3) \cdot \left( \frac{W}{h} + 0.264 \right)}{(\epsilon_{\text{reff}} - 0.258) \cdot \left( \frac{W}{h} - 0.8 \right)} \quad (4)$$

Therefore, the length of the radiating patch is obtained by

$$L = L_{\text{eff}} - 2\Delta L \quad (5)$$

Length of ground,  $L_g$  is calculated by

$$L_g = 6h + L \quad (6)$$

The width of the ground,  $W_g$  is calculated by

$$W_g = 6h + W \quad (7)$$

The slot, patch shape and feed width of the antenna design parameters are researched and compared to obtain the best impedance bandwidth and return loss performance. Numerous techniques have been developed to increase the bandwidth including cutting the slot, decreasing the substrate permittivity and increasing patch height [6]. The paper showed that the slotted patch antenna has a better impedance bandwidth than the non-slotted patch. Higher impedance of bandwidth enables the improvement of noise suppression and facilitates PD location [7]. The increasing of slot width resulting in the resonant structure of the antenna becomes weaker than the return loss value is getting poorer. Then, the increasing of slot length will lower the resonant which the size of the microstrip patch will be reduced.

The modification of the ground plane obtains the enhancement of bandwidth. For further improvement, the top corners of the ground are removed and resulted in symmetrical diagonal to enhance the bandwidth. By using a UWB antenna for PD detection techniques, the specific characteristic of PD can be detected, observed and understood more for exact investigations of the damage process and behavior of aging in the insulation [8]. The FR-4 ( $\epsilon_r = 4.7$ ) is chosen as the substrate of this antenna due to hardness, low cost and easily available.

### 2.1. Ultra Wide Band Antennas (UWB-1 & UWB-2)

The parameters for a UWB-1 microstrip patch antenna including calculation, slotting technique, and creation of waveguide port is designed by using CST Studio Suite. The basic parameters of length and width of the radiating patch, substrate and ground plane are calculated by using the formulas (1) - (7). For UWB-1, the operating frequency is at 800MHz. A slanted structure at both sides of the radiating patch is developed to get a wider impedance bandwidth. Hence, the operating bands for the antenna can obtain a good impedance matching across it.

Next, the operating frequency for the proposed UWB-2 antenna is 500MHz. Therefore, the size of the patch for UWB-2 is bigger than UWB-1. The higher the operating frequency, the smaller the size of the patch of the printed antenna. The methods included in designing the proposed UWB-2 antenna to enhance the bandwidth of the antenna performance are a modification of ground, slotting patch and slanting patch techniques. The schematic configuration of the UWB-1 and UWB-2 are shown in Figures 2 and 3. Proposed parameter specifications are given in Table 1.

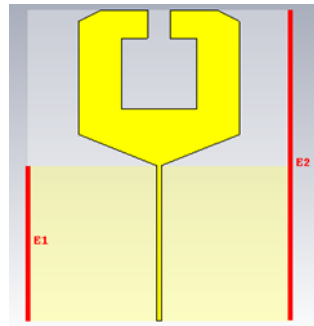


**Figure 2.** Schematic configuration of the proposed UWB\_1.

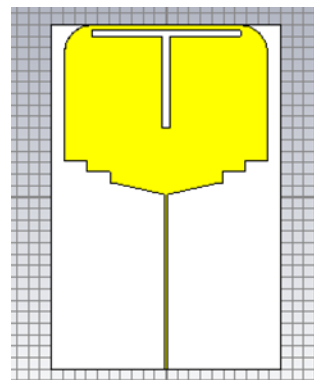


**Figure 3.** Schematic configuration of the proposed UWB\_2.

**Table 1.** Parameters of the proposed antennas.

Parameters	UWB_1	UWB_2
The dielectric constant of the dielectric substrate, $\epsilon_r$	4.7	4.7
The thickness of the dielectric substrate, h	1.60 mm	1.60 mm
Length of the radiating patch, L	86.00 mm	138.28 mm
The width of the radiating patch, W	111.00 mm	177.70 mm
Length of the dielectric substrate, Ls	215.00 mm	300.00 mm
The width of the dielectric substrate, Ws	182.00 mm	200.00 mm
Length of ground, Lg	107.50 mm	151.72 mm
The width of the ground, Wg	182.00 mm	200.00 mm
Length of microstrip feed, Lf	107.00 mm	151.72 mm
The width of the microstrip feed, Wf	3.00 mm	3.00 mm

The bandwidth from the simulated S11 result of UWB\_1 is 1.009 GHz at the point -10dB, which is from 0.463 GHz to 1.472 GHz is shown in Figure 4.

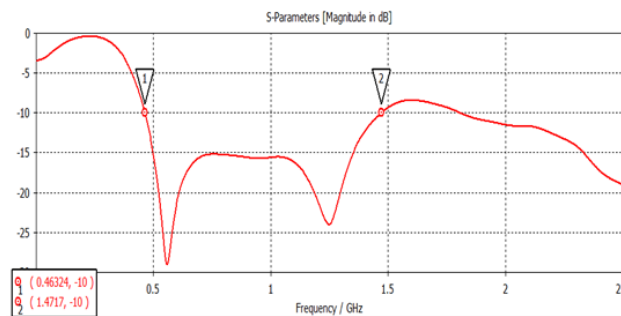


**Figure 4.** Simulated S11 of the proposed UWB\_1.

With both slots and cutting at the corner of upper and bottom radiating patch, the performance of return loss, S11 fall at the desired dB and resonant frequency as shown in Figure 5., bandwidth from 0.339 GHz to 1.197 GHz, (Bandwidth = 0.858 GHz) at -10dB respectively.

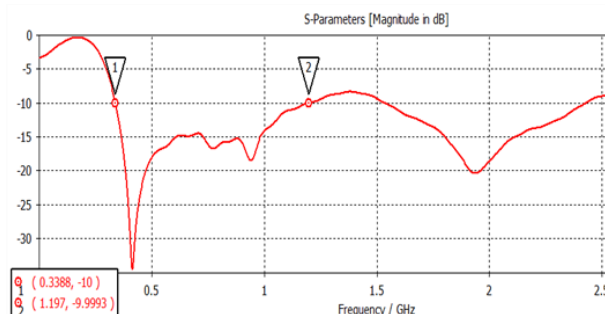


**Figure 5.** Simulated S11 of the proposed UWB\_2.

### 3. Experimental Procedure

The schematic diagram in Figure 6 shows the experimental set up of the UHF partial discharge detection. The fabricated UWB\_1, UWB\_2, and Doble’s whip antenna are located near the test cell of needle-to-sphere gap in 30 minutes measurement duration at a different time with the same level of voltage applied at 18 kV. The distance between the antenna and the needle sphere gap is fixed at 25 cm, and the distance between the needle and the sphere gap is 40 mm.

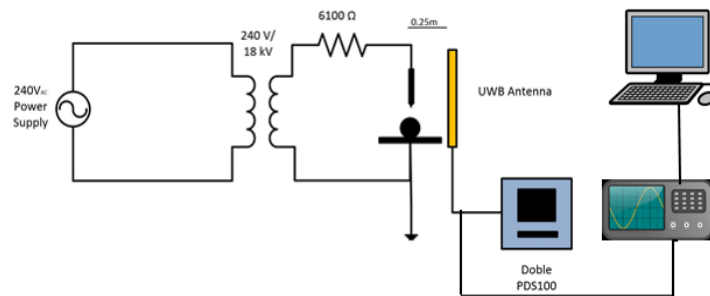
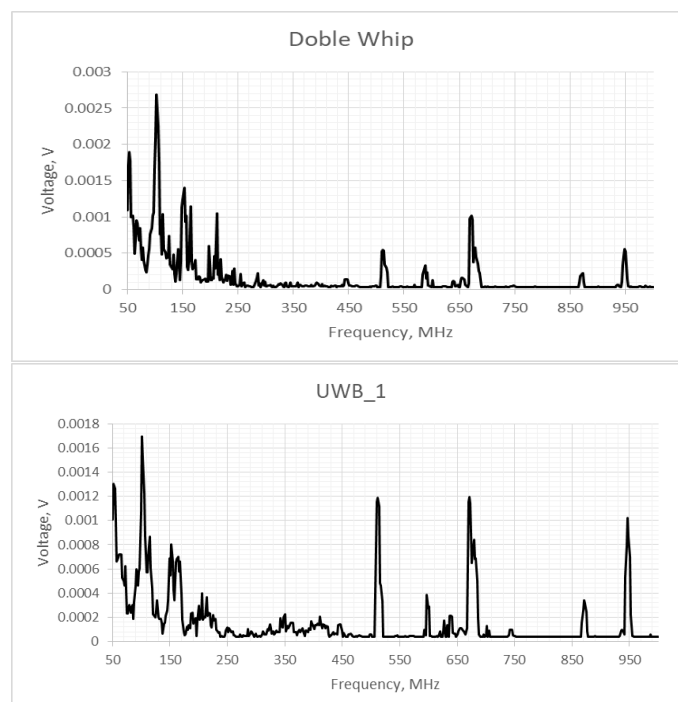


**Figure 6.** Schematic diagram of the PD detection circuit with the proposed antenna.

The Doble PDS-100 was used for this experiment is a portable tool that allows the detection of partial discharge sources in a simple and non-invasive way. It does this through the detection of radio frequency signals that emit these phenomena. This method of detection is very advantageous since it is non-invasive, and it allows the detection of PD in high voltage.

### 4. Result And Discussion

Before the high voltage application for this PD detection, the background noise is measured. The background noise measurement is done by measuring the voltage amplitude in the absence of 18 kV applied voltage. Then, the voltage is raised to 18 kV, and the PD pulses are synchronized with the trigger set to the oscilloscope where the antenna is connected. The voltage peak of the Doble Whip, UWB\_1 and UWB\_2 is 2.682 mV, 1.693 mV, and 1.634 mV respectively as given in Figure 7.



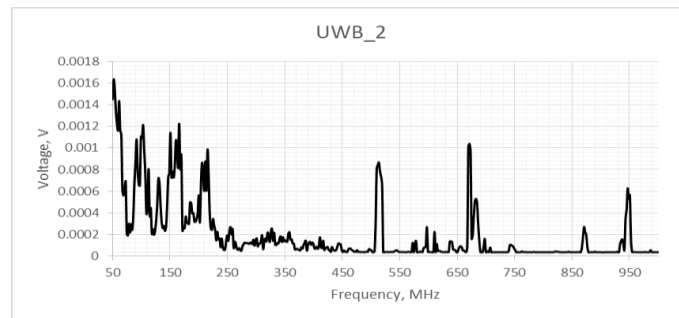


**Figure 7.** FFT voltage amplitude for PD at 18 kV. Top : Doble whip antenna (commercial); Middle UWB\_1 antenna; Bottom : UWB\_2 antenna.

Table 2 briefly discusses the detected PD power level detected from the antennas by showing the cumulative power by bands. The frequency response of the antenna is divided into three ranges of frequency from 50 to 300 MHz, from 300 to 600 MHz and from 600 MHz to 1000 MHz. The table below represents the ratio between the power content in squared volts with PD and without PD. The best frequency response is in the lower frequency, range from 50 to 300 MHz. It can be assuredly seen that the spectral power of the PD pulses detected has a higher voltage than in other frequency ranges. In higher frequency ranges of 300 to 600 MHz and 600 to 1000 MHz, the cumulative power is quite low due to the low PD activity. The UWB\_2 is founded the best behavior PD detection at 50 to 300 MHz according to the ratio calculated 158.387, followed by Doble Whip, 141.080 and UWB\_1, 71.282.

**Table 2.** Cumulative power by bands.

Antenna	Section	Cumulative power by bands (V <sup>2</sup> )		Ratio
		0 kV	18 kV	
<b>Doble's Whip</b>	1	2.629e-5	3.709e-3	141.080
	2	3.518e-5	1.219e-4	3.465
	3	6.217e-5	2.760e-4	4.439
<b>UWB_1</b>	1	2.629e-5	1.874e-3	71.282
	2	3.518e-5	2.872e-4	8.164
	3	6.217e-5	4.991e-4	8.028
<b>UWB_2</b>	1	2.629e-5	4.164e-3	158.387
	2	3.518e-5	3.079e-4	8.752
	3	6.217e-5	3.296e-4	5.302

Three measurements were carried out with the PDS-100 corresponding to the three frequency ranges mentioned in previous to measure in greater detail of the areas in which it is believed that PD will most likely appear. The analyzation of the graph offered by the spectrum analyzer is as shown in Figure 8. The red spectrum corresponds to the noise, and the green, blue and yellow spectrum correspond to the activity related to the internal PD detected by Doble's whip antenna, UWB\_1 antenna, and UWB\_2 antenna respectively. The accumulated values in each section frequency range are divided among themselves to obtain a ratio as tabulated in Table 3. The ratio indicates the difference that occurs between the noise signals and the activity corresponding to the PD activity. The highest ratio occurs in the section from 50 MHz to 300 MHz due to the internal PDs usually occur around 150 MHz and 250 MHz.



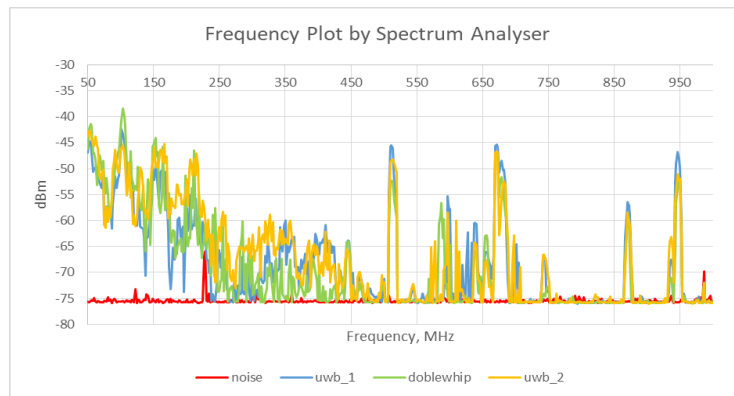


**Figure 8.** Frequency plot by a spectrum analyzer.

**Table 3.** The ratio for partial discharge detection.

Section	Frequency range (MHz)	Cumulative noise (dBm)	Cumulative internal PD (dBm)	Ratio
<b>Doble’s whip</b>				
1	50 – 300	-10025.9	-7821.73	1.2818
2	300 – 600	-9514.47	-11440.2	0.8316
3	600 – 1000	-15858.1	-15363.9	1.0322
<b>UWB_1</b>				
1	50 – 300	-10025.9	-8129.47	1.2333
2	300 – 600	-9514.47	-11020.3	0.8634
3	600 – 1000	-15858.1	-15119.5	1.0489
<b>UWB_2</b>				
1	50 – 300	-10025.9	-7480.34	1.3403
2	300 – 600	-9514.47	-10937.2	0.8699
3	600 - 1000	-15858.1	-15212.8	1.0424

The detection of the PD pulses detected by commercial Doble’s whip antenna and both fabricated UWB\_1 and UWB\_2 antennas are almost the same. The fabricated UWB\_1 and UWB\_2 antennas are proven that both planar antennas can detect PD pulses and the measurement data from them are slightly the same with the commercial PD detector. From Figure 9, it shows that the PD pulses detected from the applied voltage are in the range of -120 pC to 200 pC.

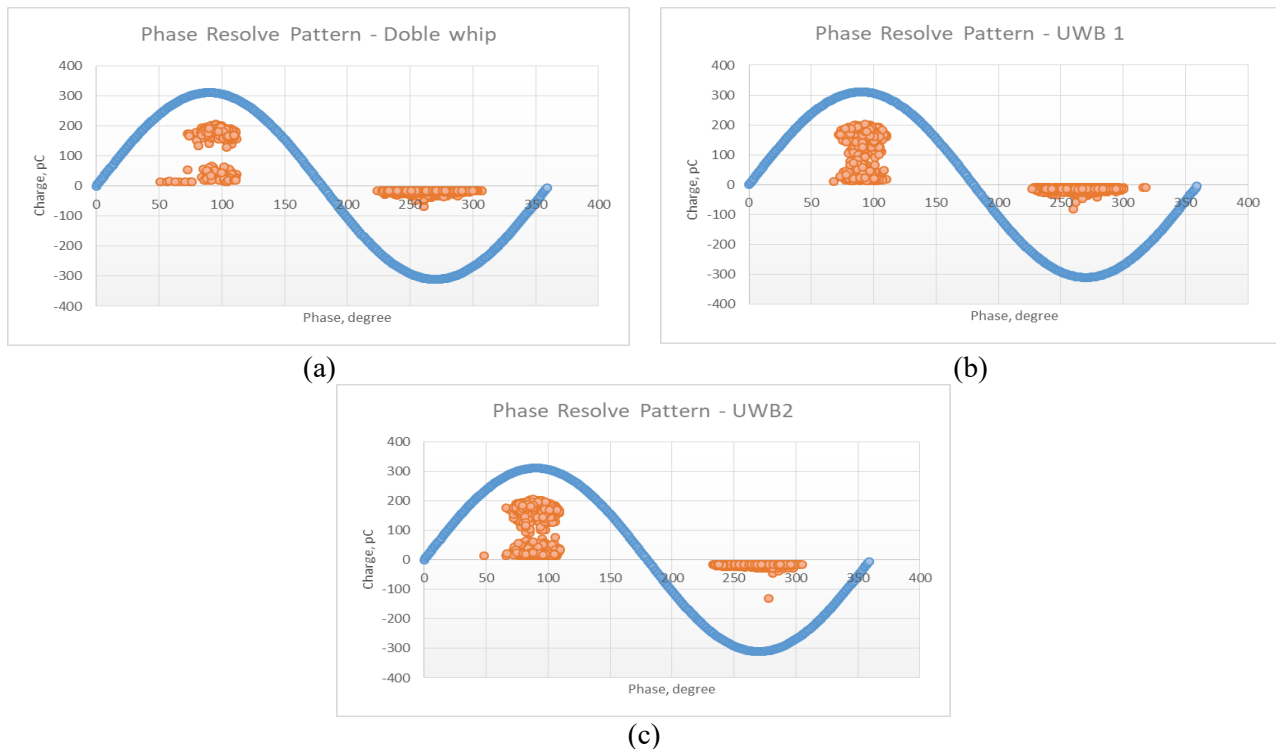


**Figure 9.** Partial discharge phase resolve pattern; (a) PRPD comparable to Doble's whip antenna, (b) PRPD comparable to UWB1 antenna, and (c) PRPD comparable to UWB2 antenna.

## 5. Conclusion

In this paper, UWB antennas for PD UHF detection in high voltage equipment are designed and implemented. The design of both UWB\_1 and UWB\_2 are optimized through a simulation study by using CST Studio Suite. The detection and measurement of PD UHF signals showed that the fabricated antennas could detect the UHF PD signals appropriately. Therefore, the proposed UWB antennas are well suited for UHF PD online monitoring due to the good performance of UHF PD detection during the laboratory experiments were carried out.

## 6. Acknowledgment

Authors would like to acknowledge Universitas Sriwijaya and Universiti Teknologi Malaysia for giving financial sponsorship and research facilities through a research grant, under the numbers of 4B278, 4B279, 4B340, 4B342 and 13H98.

## References

- [1] Neumann, C Krampe, B Feger, R Feser, K Knapp, M Breuer, A Rees 2000 PD measurements on GIS of different designs by non-conventional UHF sensors, *CIGER session 15–305*, 1–9.
- [2] Dustin Ashliegh 2015 A Guide to Understanding Partial Discharge Sensor Applications, [online] retrieved from <https://www.linkedin.com/pulse/guide-understanding-partial-discharge-sensor-dustin-ashliegh>
- [3] M Hikita, S Ohtsuka, and S Matsumoto 2007 Recent trend of the partial discharge measurement technique using the UHF electromagnetic wave detection method, *IEEJ Transactions on Electrical and Electronic Engineering*, vol. **2**, no. 5. pp. 504–509.
- [4] Z N Yaacob M M, Alsaedi M A, AL Gizi Abdullah 2013 Partial discharge signal detection using the ultra-high-frequency method in high voltage power Equipment: A review, *Int. J. Sci. Eng. Res.*, vol. **4**, no. 1, pp. 283–286.
- [5] G Robles *et al.* 2013 On the use of Vivaldi antennas in the detection of partial discharges, in

- Proceedings of IEEE International Conference on Solid Dielectrics, ICSD*, pp. 302–30.
- [6] L C Ping, C K Chakrabarty, and R A Khan 2009 Design of ultra-wideband slotted microstrip patch antenna, in *Proceedings - MICC 2009: 2009 IEEE 9th Malaysia International Conference on Communications with a Special Workshop on Digital TV Contents*, pp. 41–45.
- [7] B Sarkar, D K Mishra, C Koley, and N K Roy 2014 Microstrip patch antenna based UHF sensor for detection of Partial Discharge in High Voltage electrical equipment, in *11th IEEE India Conference: Emerging Trends and Innovation in Technology, INDICON 2014*.
- [8] G Robles *et al.* 2012 Antenna selection and frequency response study for UHF detection of partial discharges, *IEEE Int. Instrum. Meas. Technol. Conf.*, pp. 1496–1499.